Iron–Iridium Mixed-Metal Carbonyl Clusters. 4.[1] Synthesis, Characterization, and Chemical Behavior of $[FeIr_4(CO)_{13}]^{2-}$ and $[Fe_2Ir_4(CO)_{16}]^{2-}$. Solid-State Structures of $[PPh_4]_2[FeIr_4(CO)_{13}]\cdot C_4H_8O$ and $[NEt_4][NMe_3(CH_2Ph)][Fe_2Ir_4(CO)_{16}]$

Roberto Della Pergola,*[2a] Alessandro Ceriotti,[2a] Luigi Garlaschelli,[2a] Francesco Demartin,[2b] Mario Manassero,[2b] Norberto Masciocchi,*[2b] and Mirella Sansoni[2b]

Dipartimento di Chimica Inorganica, Metallorganica e Analitica and Istituto di Chimica Strutturistica Inorganica, Università degli Studi di Milano, Via G. Venezian 21, 20133 Milano, Italy

Received December 8, 1992

The cluster $[FeIr_4(CO)_{13}]^{2-}$ is obtained by decarbonylation of $[FeIr_4(CO)_{15}]^{2-}$, either at room temperature or by moderate heating of a solution of the complex. The salt $[PPh_4]_2[FeIr_4(CO)_{13}]\cdot C_4H_8O$ crystallizes in the triclinic space group $P\bar{1}$ (No. 2), with a = 11.337(4) Å, b = 13.105(4) Å, c = 23.306(6) Å, α = 100.04(2)°, β = 97.99(2)°, γ = 106.68(2)°, V = 3200(4) Å^3, and Z = 2. The structure was solved and refined by full-matrix least-squares methods down to R = 0.050 and R_w = 0.053 for 3914 independent reflections with $I \geq 3\sigma(I)$. The anion consists of a trigonal bipyramidal metal frame with the iron located in the apical position; the apical and equatorial metal atoms are connected by short bond distances, as commonly observed in bipyramidal clusters having 72 cluster valence electrons. Average metal–metal bond distances (Å): Ir_{eq}–Ir_{eq} = 2.748, Ir_{ap}–Ir_{eq} = 2.735, Fe_{ap}–Ir_{eq} = 2.670. The cluster $[Fe_2Ir_4(CO)_{16}]^{2-}$ may be obtained by condensation of $[Fe_2(CO)_8]^{2-}$ or $[Fe(CO)_4]^{2-}$ onto $Ir_4(CO)_{12}$. The salt $[NEt_4][NMe_3(CH_2Ph)][Fe_2Ir_4(CO)_{16}]$ crystallizes in the monoclinic space group $P2_1/c$ (No. 14), with a = 10.763(2) Å, b = 20.525(3) Å, c = 19.345(3) Å, β = 97.36(1)°, V = 4238(2) Å^3, and Z = 4. The structure was solved and refined by full-matrix least-squares methods down to R = 0.041 and R_w = 0.047 for 3624 independent reflections with $I \geq 3\sigma(I)$. The anion consists of an almost regular octahedron of metal atoms, adopting a ligand architecture with four asymmetric face-bridging and twelve terminal carbonyl ligands. From the X-ray data the isomer with the iron atoms *trans* to each other was found to be prevalent (>80%), but the exact ratio between the *cis* and *trans* isomers could not be evaluated. The cluster ideally belongs to the S_4 point group of symmetry. The average metal–metal distance is 2.747 Å.

Introduction

As part of our continuing interest in Fe–Ir carbonyl clusters, we have previously described the synthesis, the chemical behavior, and the solid-state structures of clusters containing four, five, and six metal atoms, with the Fe:Ir ratio varying from 0.2 to 3.[1,3,4] In these papers we omitted the description of two other compounds, which had already been detected but lacked complete characterization. The formulas of the two clusters $[FeIr_4(CO)_{13}]^{2-}$ (**1**) and $[Fe_2Ir_4(CO)_{16}]^{2-}$ (**2**) were subsequently determined, and their chemical reactivities were tested. Eventually, we were able to devise tailored syntheses for these derivatives, which allowed their preparation in large amounts and, consequently, a full investigation through a combination of various analytical and diffractometric methods.

In the future, we will focus our attention on the spectroscopic and catalytic properties of these clusters, rather than on synthetic aspects, since the cluster $[Fe_2Ir_4(CO)_{16}]^{2-}$ has been found to be a valuable precursor for supported bimetallic particles in the heterogeneous hydrogenation of carbon monoxide.[5]

Results

1. Synthesis of the Anions $[FeIr_4(CO)_{13}]^{2-}$ (1) and $[Fe_2Ir_4(CO)_{16}]^{2-}$ (2). As already reported, the degradation of the yellow dianion $[FeIr_4(CO)_{15}]^{2-}$ (**3**) under atmospheric pressure of carbon monoxide produces the tetranuclear cluster $[FeIr_3(CO)_{12}]^-$,[4] along with the mononuclear complex $[Ir(CO)_4]^-$, according to eq 1. Complex **3**, however, is not stable even under

$$[FeIr_4(CO)_{15}]^{2-} + CO \rightarrow [FeIr_3(CO)_{12}]^- + [Ir(CO)_4]^- \quad (1)$$

nitrogen and, when kept in solution, is mainly transformed into a darker species, characterized as the dianion $[FeIr_4(CO)_{13}]^{2-}$ (**1**); the decarbonylation process is remarkably slow at room temperature and is completed after about 3 days. Additionally, significant amounts of $[FeIr_3(CO)_{12}]^-$ and $[Ir(CO)_4]^-$ are also formed. It seems reasonable to deduce that the CO evolved from reaction 2 reacts with $[FeIr_4(CO)_{15}]^{2-}$ according to eq 1. In

$$[FeIr_4(CO)_{15}]^{2-} \rightarrow [FeIr_4(CO)_{13}]^{2-} + 2CO \quad (2)$$

order to avoid this undesired side reaction as much as possible, the inert atmosphere over the solution of **3** is frequently renewed by freeze–pump–thaw cycles.

A more selective and much faster synthesis of **1** can be accomplished by moderate heating of **3** in refluxing acetone. The side reaction is markedly reduced but not completely suppressed, and the desired dianion $[FeIr_4(CO)_{13}]^{2-}$ is obtained in high yield after about 1 h.

The reverse reaction of (2) is fast, and $[FeIr_4(CO)_{15}]^{2-}$ is regenerated within a few minutes when **1** is submitted to an atmospheric pressure of CO.

The anion $[Fe_2Ir_4(CO)_{16}]^{2-}$ (**2**) was originally observed as a major product of the redox condensation of $Na_2[Fe(CO)_4]$ and

(1) Part 3: Ceriotti, A.; Della Pergola, R.; Garlaschelli, L.; Laschi, F.; Manassero, M.; Masciocchi, N.; Sansoni, M.; Zanello, P. *Inorg. Chem.* **1991**, *30*, 3349.
(2) (a) Dipartimento di Chimica Inorganica, Metallorganica e Analitica. (b) Istituto di Chimica Strutturistica Inorganica.
(3) Della Pergola, R.; Garlaschelli, L.; Demartin, F.; Manassero, M.; Masciocchi, N.; Sansoni, M.; Fumagalli, A. *J. Chem. Soc., Dalton Trans.* **1989**, 1109.
(4) Della Pergola, R.; Garlaschelli, L.; Demartin, F.; Manassero, M.; Masciocchi, N.; Sansoni, M. *J. Chem. Soc., Dalton Trans.* **1990**, 127.
(5) (a) Marengo, S.; Psaro, R.; Dossi, C.; Della Pergola, R.; Garlaschelli, L.; Minotti, E.; Zanderighi, G. M. Paper presented at the VIIIth National Congress on Catalysis, Rimini, Italy, Sept 30–Oct 2, 1992. (b) Ichikawa, M. *Adv. Catal.* **1992**, *38*, 283.

0020-1669/93/1332-3277$04.00/0

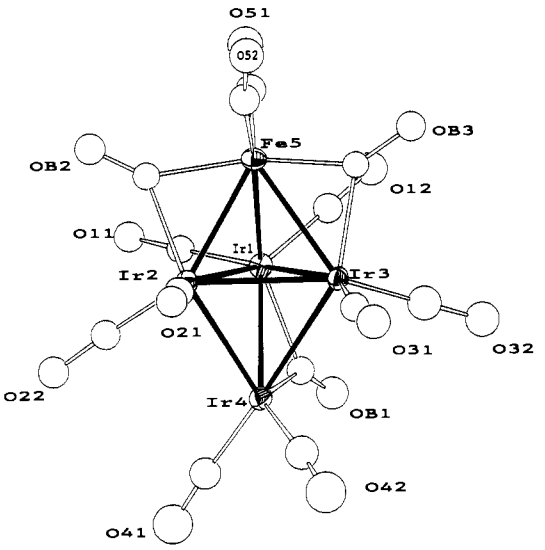

Figure 1. ORTEP drawing and atom-labeling scheme for $[FeIr_4(CO)_{13}]^{2-}$. Thermal ellipsoids are drawn at 30% probability. Carbonyl carbons are designated in a manner analogous to the oxygens to which they are attached.

$Ir_4(CO)_{12}$ (molar ratio 4:1) in refluxing thf. In combination with a suitable counterion, crystals of sufficient quality for X-ray data collection were eventually obtained. The cluster was identified as $[Fe_2Ir_4(CO)_{16}]^{2-}$, and thereafter, more rational syntheses were devised. In principle, $[Fe_2Ir_4(CO)_{16}]^{2-}$ can be obtained by condensation of iron pentacarbonyl onto **1** or **3**: the reaction does indeed proceed, but other byproducts, mainly $[Fe_2Ir_2(CO)_{12}]^{2-}$, of similar solubility are also formed.[4] Thus, the purification of **2** would require a complicated workup, and this method was considered inconvenient and therefore abandoned. On the contrary, good results were obtained on heating an equimolar mixture of $[Fe_2(CO)_8]^{2-}$ and $Ir_4(CO)_{12}$ in acetonitrile under reflux, according to eq 3.

$$Ir_4(CO)_{12} + [Fe_2(CO)_8]^{2-} \rightarrow [Fe_2Ir_4(CO)_{16}]^{2-} + 4CO \quad (3)$$

The two methods reported here, involving the use of iron carbonyl anions, can be performed with small tetraalkylammonium cations, such as $[NEt_4]^+$ or $[NMe_3(CH_2Ph)]^+$, and many different salts, of high purity and identical properties, can be obtained easily from the reaction mixtures.

Complex **2** has an unexpected chemical inertness and does not react with CO, even after prolonged standing; under weak protonating conditions (H_3PO_4 in acetone) we could monitor only a slow decomposition, with the formation of small amounts of $Fe(CO)_5$, but most of the cluster survived intact. This behavior is in sharp contrast with that reported for the analogous $[Fe_2Rh_4(CO)_{16}]^{2-}$, which is oxidized by acids to $[FeRh_5(CO)_{16}]^-$ and rapidly degraded by CO to $[FeRh_4(CO)_{15}]^{2-}$ and $Fe(CO)_5$.[6]

2. Crystal Structure of $[PPh_4]_2[FeIr_4(CO)_{10}(\mu\text{-}CO)_3)]\cdot C_4H_8O$ (1a). The crystal structure of **1a** consists of an ionic packing of tetraphenylphosphonium cations, complex **1** anions, and incorporated thf molecules. Relevant bond distances and angles for the anion are collected in Table I. An ORTEP drawing of **1** is depicted in Figure 1.

The metal skeleton of $[FeIr_4(CO)_{13}]^{2-}$ consists of a trigonal bipyramid, with the iron atom located in the apical position. Each metal atom is bonded to two terminal carbonyl ligands, while, of the three edge bridging CO's, two span Ir–Fe edges and one spans an Ir_{eq}–Ir_{ap} bond; however, because of a significant twist in the bridging ligand attached to the apical Ir(4) atom [C(B1)–O(B1)], the whole anion does not possess any idealized symmetry element at all. The Ir–Ir bonds in the equatorial plane (average 2.748 Å) are longer than those found in $[FeIr_4(CO)_{15}]^{2-}$ and $[Fe_2Ir_3(CO)_{14}]^-$ (average 2.708 Å for both anions);[3] on the contrary, the apical-to-equatorial Ir–Ir interactions (average 2.735 Å) are about 0.25 Å shorter in $[FeIr_4(CO)_{13}]^{2-}$ than in $[FeIr_4(CO)_{15}]^{2-}$ (see Table II), as expected for a 72, rather than 76, cluster valence electron (CVE) compound, while the average Ir–Fe distance in **1** of 2.670 Å is comparable with that observed in $[Fe_2Ir_3(CO)_{14}]^-$ (2.646 Å). Moreover, a significant shortening of the metal–metal distances is observed when bridging CO's are present, for both the Ir–Ir and Ir–Fe cases: $Ir\text{–}Ir_{bridged}$ = 2.69 Å, $Ir\text{–}Ir_{unbridged}$(av) = 2.76 Å, $Fe\text{–}Ir_{bridged}$(av) = 2.62 Å, $Fe\text{–}Ir_{unbridged}$ = 2.76 Å.

Metal–C bond distances range from 1.67(4) to 1.86(3) Å for terminal carbonyl ligands and from 1.87(3) to 2.09(3) Å for edge-bridging ligands; the corresponding average M–C–O angles are 175 and 139°, respectively.

3. Crystal Structure of $[NEt_4][NMe_3(CH_2Ph)][Fe_2Ir_4(CO)_{12}(\mu_3\text{-}CO)_4]$ (2a). The crystal structure of **2a** consists of an ionic packing of tetraalkylammonium cations and complex **2** ions, with

Table I. Relevant Bond Distances (Å) and Angles (deg) for $[FeIr_4(CO)_{13}]^{2-}$ (**1**) with Estimated Standard Deviations (Esd's) in Parentheses

Metal–Metal			
Ir(1)–Ir(2)	2.779(2)	Ir(3)–Ir(4)	2.773(2)
Ir(1)–Ir(3)	2.704(1)	Ir(1)–Fe(5)	2.758(4)
Ir(2)–Ir(3)	2.761(1)	Ir(2)–Fe(5)	2.578(4)
Ir(1)–Ir(4)	2.690(2)	Ir(3)–Fe(5)	2.673(4)
Ir(2)–Ir(4)	2.741(2)		
Metal–CO			
Ir(1)–C(11)	1.85(2)	Fe(5)–C(51)	1.67(3)
Ir(1)–C(12)	1.85(3)	Fe(5)–C(52)	1.67(4)
Ir(2)–C(21)	1.86(3)	Ir(1)–C(B1)	2.09(3)
Ir(2)–C(22)	1.81(3)	Ir(4)–C(B1)	1.97(3)
Ir(3)–C(31)	1.67(2)	Ir(2)–C(B2)	2.09(3)
Ir(3)–C(32)	1.76(4)	Fe(5)–C(B2)	1.97(3)
Ir(4)–C(41)	1.81(4)	Ir(3)–C(B3)	2.09(3)
Ir(4)–C(42)	1.82(3)	Fe(5)–C(B3)	1.87(3)
C–O			
C(11)–O(11)	1.18(3)	C(42)–O(42)	1.13(4)
C(12)–O(12)	1.19(4)	C(51)–O(51)	1.18(4)
C(21)–O(21)	1.13(4)	C(52)–O(52)	1.21(4)
C(22)–O(22)	1.20(4)	C(B1)–O(B1)	1.15(4)
C(31)–O(31)	1.28(3)	C(B2)–O(B2)	1.13(4)
C(32)–O(32)	1.20(5)	C(B3)–O(B3)	1.23(4)
C(41)–O(41)	1.16(5)		
Metal–C–O			
Ir(1)–C(11)–O(11)	178(3)	Fe(5)–C(51)–O(51)	175(3)
Ir(1)–C(12)–O(12)	177(3)	Fe(5)–C(52)–O(52)	172(3)
Ir(2)–C(21)–O(21)	176(3)	Ir(1)–C(B1)–O(B1)	134(2)
Ir(2)–C(22)–O(22)	177(3)	Ir(4)–C(B1)–O(B1)	143(2)
Ir(3)–C(31)–O(31)	172(3)	Ir(2)–C(B2)–O(B2)	135(2)
Ir(3)–C(32)–O(32)	178(3)	Fe(5)–C(B2)–O(B2)	145(3)
Ir(4)–C(41)–O(41)	175(3)	Ir(3)–C(B3)–O(B3)	133(2)
Ir(4)–C(42)–O(42)	174(3)	Fe(5)–C(B3)–O(B3)	142(2)

Table II. Synoptic Collection of Relevant Bonding Parameters of the Trigonal Bipyramidal Metal Core of Pentanuclear Fe–Ir Clusters[a]

	cluster		
parameter	$[FeIr_4(CO)_{13}]^{2-}$	$[FeIr_4(CO)_{15}]^{2-}$	$[Fe_2Ir_3(CO)_{14}]^-$
$\langle Ir_{eq}\text{–}Ir_{eq}\rangle$	2.748	2.708	2.708
$\langle Ir_{ap}\text{–}Ir_{eq}\rangle$	2.735	2.991	
$\langle Fe_{ap}\text{–}Ir_{eq}\rangle$	2.670	2.943	2.646
$M_{ap}\text{–}M_{ap}$	4.37	5.04	4.27
symmetry[b]	C_1	C_s	C_2
no. of CVE's	72	76	72

[a] Typical esd's on the single values are 0.001–0.002 Å. [b] Including carbon monoxide groups.

(6) (a) Ceriotti, A.; Longoni, G.; Manassero, M.; Sansoni, M.; Della Pergola, R.; Heaton, B. T.; Smith, D. O. *J. Chem. Soc., Chem. Commun.* **1982**, 886. (b) Ceriotti, A.; Longoni, G.; Della Pergola, R.; Heaton, B. T.; Smith, D. O. *J. Chem. Soc., Dalton Trans.* **1983**, 1941.

Table III. Relevant Bond Distances (Å) and Angles (deg) for $[Fe_2Ir_4(CO)_{16}]^{2-}$ (**2**) (Esd's in Parentheses)

Metal–Metal			
Ir(1)–Ir(2)	2.768(1)	Ir(3)–Fe(6)	2.692(2)
Ir(2)–Ir(3)	2.751(1)	Ir(4)–Fe(6)	2.734(2)
Ir(3)–Ir(4)	2.777(1)	Ir(1)–Fe(5)	2.794(2)
Ir(1)–Ir(4)	2.733(2)	Ir(2)–Fe(5)	2.703(2)
Ir(1)–Fe(6)	2.725(2)	Ir(3)–Fe(5)	2.771(2)
Ir(2)–Fe(6)	2.753(2)	Ir(4)–Fe(5)	2.765(2)
Metal–CO			
Ir(1)–C(11)	1.92(2)	Ir(1)–C(B1)	2.18(2)
Ir(1)–C(12)	1.91(2)	Fe(6)–C(B1)	1.98(2)
Ir(2)–C(21)	1.90(3)	Ir(2)···C(B1)	2.51(2)
Ir(2)–C(22)	1.84(2)	Ir(4)–C(B2)	2.09(2)
Ir(3)–C(31)	1.83(2)	Fe(5)–C(B2)	2.11(2)
Ir(3)–C(32)	1.85(2)	Ir(1)···C(B2)	2.43(3)
Ir(4)–C(41)	1.85(3)	Ir(2)–C(B3)	2.17(2)
Ir(4)–C(42)	1.71(3)	Fe(5)–C(B3)	1.92(3)
Fe(5)–C(51)	1.76(2)	Ir(3)···C(B3)	2.53(2)
Fe(5)–C(52)	1.72(3)	Ir(3)–C(B4)	2.17(2)
Fe(6)–C(61)	1.84(2)	Fe(6)–C(B4)	2.00(2)
Fe(6)–C(62)	1.82(2)	Ir(4)···C(B4)	2.33(2)
C=O			
C(11)–O(11)	1.09(3)	C(51)–O(51)	1.13(3)
C(12)–O(12)	1.11(4)	C(52)–O(52)	1.15(3)
C(21)–O(21)	1.05(3)	C(61)–O(61)	1.07(3)
C(22)–O(22)	1.14(3)	C(62)–O(62)	1.09(3)
C(31)–O(31)	1.14(3)	C(B1)–O(B1)	1.14(3)
C(32)–O(32)	1.14(3)	C(B2)–O(B2)	1.21(3)
C(41)–O(41)	1.11(3)	C(B3)–O(B3)	1.20(3)
C(42)–O(42)	1.25(4)	C(B4)–O(B4)	1.17(2)
Metal–C–O			
Ir(1)–C(11)–O(11)	172(2)	Fe(6)–C(61)–O(61)	176(2)
Ir(1)–C(12)–O(12)	179(2)	Fe(6)–C(62)–O(62)	176(2)
Ir(2)–C(21)–O(21)	176(3)	Ir(1)–C(B1)–O(B1)	132(2)
Ir(2)–C(22)–O(22)	174(2)	Fe(6)–C(B1)–O(B1)	142(2)
Ir(3)–C(31)–O(31)	175(2)	Ir(4)–C(B2)–O(B2)	135(2)
Ir(3)–C(32)–O(32)	178(2)	Fe(5)–C(B2)–O(B2)	135(2)
Ir(4)–C(41)–O(41)	178(2)	Ir(2)–C(B3)–O(B3)	130(2)
Ir(4)–C(42)–O(42)	179(2)	Fe(5)–C(B3)–O(B3)	142(2)
Fe(5)–C(51)–O(51)	179(2)	Ir(3)–C(B4)–O(B4)	130(2)
Fe(5)–C(52)–O(52)	176(2)	Fe(6)–C(B4)–O(B4)	140(2)

normal van der Waals contacts. Relevant bond distances and angles for anion **2** are collected in Table III.

The $[Fe_2Ir_4(CO)_{16}]^{2-}$ anion contains an almost regular mixed-metal octahedron, with the two iron atoms mostly located in a *trans* position; neither the presence of a small amount of the *cis* isomer, nor the *cis*:*trans* ratio could be assessed from the available structural data (see Experimental Section). An ORTEP drawing of **2** is depicted in Figure 2.

The average metal–metal distance (2.747 Å) is comparable to that of the isostructural $[FeIr_5(CO)_{16}]^-$ (2.773 Å) and its related $[FeIr_5(CO)_{15}]^{3-}$ (2.767 Å) and $[HFeIr_5(CO)_{15}]^{2-}$ (2.763 Å) anions,[1] while any detailed comparison of the individual metal–metal bond interactions becomes meaningless, due to the observed substitutional disorder.[1,4]

Each metal atom is connected to two terminal and to two edge-bridging ligands; however, the presence of short nonbonding Ir···C contacts (minimum 2.33 Å, maximum 2.53 Å) gives the μ-CO a significant "semitriple" character, similar to that invoked in the bridging ligands of $[Ir_6(CO)_{15}(AuPPh_3)]^-$.[7] The observed stereogeometry of the whole anion (S_4) is therefore intermediate between those observed for the red (T_d) and black (D_{2d}) isomers of $Ir_6(CO)_{16}$.[8]

Average bonding parameters for the carbonyl ligands are as follows: M–C = 1.83 Å, C–O = 1.12 Å, and M–C–O = 177°

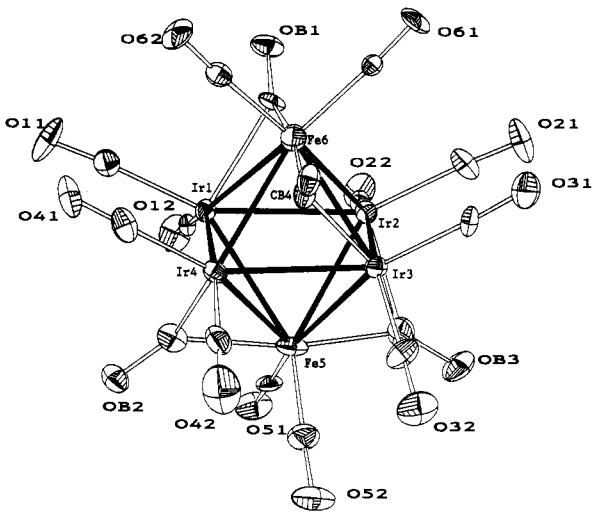

Figure 2. ORTEP drawing and atom-labeling scheme for $[Fe_2Ir_4(CO)_{16}]^{2-}$. Thermal ellipsoids are drawn at 30% probability. Carbonyl carbons are designated in a manner analogous to the oxygens to which they are attached.

(terminal CO's); M–C = 2.08 Å, C–O = 1.18 Å, and M–C–O = 136° (bridging carbonyls).

Conclusions

Pentanuclear bipyramidal mixed-metal clusters containing four atoms of Rh or Ir and one atom of Fe,[6,3] Ru,[9,10] Os,[11] or Pt[12,13] have been synthesized and their structures determined.

For $[PtRh_4(CO)_{14}]^{2-}$ and $[PtIr_4(CO)_{14}]^{2-}$, fast and fully reversible decarbonylation and carbonylation processes have been documented: the loss of two ligands is accompanied by shortening of apical–equatorial distances and by migration of the heteroatom from an equatorial to an apical position.[12,13]

All the pentanuclear clusters containing Fe, Ru, or Os possess 76 CVE's with 15 carbonyl ligands. These clusters are stable only under CO and were reported to decompose when submitted to an inert atmosphere with accompanying growth of metal frame.[10]

The decarbonylation of the dianion $[FeIr_4(CO)_{15}]^{2-}$ to $[FeIr_4(CO)_{13}]^{2-}$ involves only minor rearrangements of the cluster: the metals do not change their sites, the three bridging carbonyls, coplanar with the equatorial triangle, become terminal, and two terminal CO's are lost from the apical atoms. The stability of the "$FeIr_4$" core with 72 CVE's as $[FeIr_4(CO)_{13}]^{2-}$ and its solid state structure are new findings and can hopefully help to explain the reactivity described for related systems which undergo similar transformations.[10]

Cluster **2** represents the third member of the family of octahedral complexes $[Fe_xIr_{6-x}(CO)_{16}]^{x-}$ (x = 0–2); an analogous series has been found for Fe–Rh clusters. Dianion **2** has spectroscopic and structural similarities to the corresponding $[Fe_2Rh_4(CO)_{16}]^{2-}$. The reactivity, on the other hand, shows significant differences related to the increased inertness of octahedral iridium clusters. Structural differences are found in the ligand architecture and in the higher value of the *trans*:*cis* ratio: from ^{103}Rh NMR[6] and Mössbauer data[14] this ratio was

(7) Della Pergola, R.; Demartin, F.; Garlaschelli, L.; Manassero, M.; Martinengo, S.; Masciocchi, N.; Sansoni, M.; *Organometallics* **1991**, *10*, 2239.
(8) Garlaschelli, L.; Martinengo, S.; Bellon, P. L.; Demartin, F.; Manassero, M.; Chiang, M. Y.; Wei, C. Y.; Bau, R. *J. Am. Chem. Soc.* **1984**, *106*, 6664.
(9) Fumagalli, A.; Ciani, G.; *J. Organomet. Chem.* **1984**, *272*, 91.
(10) Fumagalli, A.; Koetzle, T. F.; Takusagawa, F. *J. Organomet. Chem.* **1981**, *213*, 365.
(11) Fumagalli, A.; Garlaschelli, L.; Della Pergola, R. *J. Organomet. Chem.* **1989**, *362*, 197.
(12) Fumagalli, A.; Martinengo, S.; Chini, P.; Galli, D.; Heaton, B. T.; Della Pergola, R. *Inorg. Chem.* **1984**, *23*, 2947.
(13) Fumagalli, A.; Della Pergola, R.; Bonacina, F.; Garlaschelli, L.; Moret, M.; Sironi, A. *J. Am. Chem. Soc.* **1989**, *111*, 165.
(14) Brint, R. P.; Collins, M. P.; Spalding, T. R.; Deeney, F. T.; Longoni, G.; Della Pergola, R. *J. Organomet. Chem.* **1987**, *319*, 219.

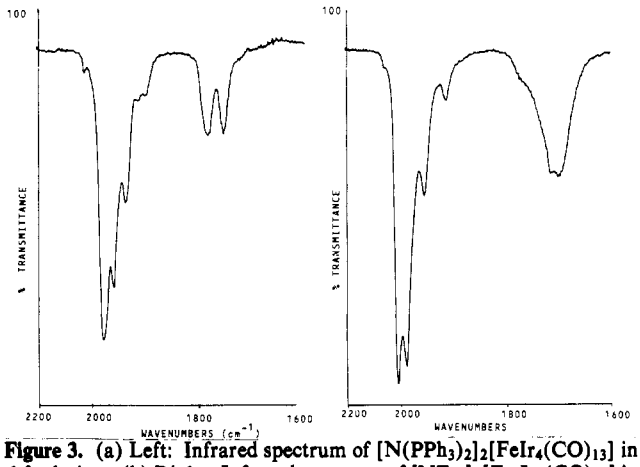

Figure 3. (a) Left: Infrared spectrum of $[N(PPh_3)_2]_2[FeIr_4(CO)_{13}]$ in thf solution. (b) Right: Infrared spectrum of $[NEt_4]_2[Fe_2Ir_4(CO)_{16}]$ in MeCN solution.

evaluated to be approximately 3 for $[Fe_2Rh_4(CO)_{16}]^{2-}$, in both solution and the solid state.

Experimental Section

All the solvents were purified and dried by conventional methods and stored under nitrogen. All the reactions were carried out under oxygen-free nitrogen or CO atmospheres using the Schlenk-tube technique.[15] $Ir_4(CO)_{12}$,[16] $Na_2[Fe(CO)]_4$,[17] $[NEt_4]_2[Fe_2(CO)_8]$,[18] and $[N(PPh_3)_2]_2[FeIr_4(CO)_{15}]$[3] were prepared by literature methods. Infrared (IR) spectra were recorded on a Perkin-Elmer 781 grating spectrophotometer using calcium fluoride cells previously purged with N_2. Samples for mass spectra were suspended in a matrix of *m*-nitrobenzyl alcohol and bombarded with a beam of Xe atoms of 70 keV with a VG Micromass machine, and the spectra were compared with computed theoretical isotope patterns; mass peaks refer to the most abundant isotopomers. Elemental analyses were carried out by the staff of the Laboratorio di Analisi of the Dipartimento di Chimica Inorganica, Metallorganica e Analitica.

Preparation of $[FeIr_4(CO)_{13}]^{2-}$ (1). $[N(PPh_3)_2]_2[FeIr_4(CO)_{15}]$ (0.22 g; 0.094 mmol) was dissolved in acetone (8 mL), and the mixture was refluxed for 1 h under a light stream of nitrogen. The progression of the reaction was monitored by IR spectroscopy, and, upon its completion, 2-propanol (15 mL) was added to the cooled solution with stirring. Partial removal of the solvent under vacuum caused the formation of a dark microcrystalline precipitate from the yellow solution. The product was collected by filtration, washed with 2-propanol, and dried. It was then extracted from the frit with tetrahydrofuran (thf) (8 mL), and the extract was layered with 2-propanol. Yield: 0.145 g (63%). FAB (negative ions): m/z = 1246 ($[FeIr_4(CO)_{15}]^-$), 1218 ($[FeIr_4(CO)_{14}]^-$), 1190 ($[FeIr_4(CO)_{13}]^-$), 1190 − 28x ($[FeIr_4(CO)_{13-x}]^-$) (x = 1–13). Anal. Calc for $C_{89}FeH_{68}Ir_4N_2O_{14}$: C, 45.69; H, 2.91; N, 1.20. Found: C, 45.92; H, 2.91; N 1.06.

The inclusion of thf in the crystals was supported by elemental analysis and confirmed by NMR. However, the crystals lost the included solvent and hence were not suitable for X-ray analysis. Crystals of the $[PPh_4]^+$ salt were obtained through a double-metathesis reaction. The first reaction was performed in acetone with stoichiometric amounts of $Na[BPh_4]$, which precipitated $[N(PPh_3)_2][BPh_4]$, leaving in solution the sodium salt of the cluster; the second reaction was carried out in MeOH; after removal of the acetone in vacuum, treatment with an excess of tetraphenylphosphonium halide precipitated $[PPh_4]_2[FeIr_4(CO)_{13}]$. Crystals of this salt were grown from thf/2-propanol. These procedures resulted in some decomposition to $[Fe_2Ir_4(CO)_{16}]^{2-}$. Change of cation did not exclude the presence of thf from the crystals, but in this case it was lost much more slowly and X-ray determination was therefore possible.

The $[N(PPh_3)_2]^+$ and $[PPh_4]^+$ salts of **1** are very soluble in acetone and acetonitrile, sparingly soluble in thf, and very insoluble in 2-propanol. IR spectrum of $[N(PPh_3)_2]_2[FeIr_4(CO)_{13}]$ (Figure 3a): ν_{CO} 2024 (vw), 1977 (vs), 1957 (s), 1934 (m), 1781 (m), 1749 (m) cm^{-1} (thf solution).

Preparation of $[Fe_2Ir_4(CO)_{16}]^{2-}$ (2). (a) $[NEt_4]_2[Fe_2(CO)_8]$ (0.32 g; 0.54 mmol) and $Ir_4(CO)_{12}$ (0.59 g; 0.55 mmol) were suspended in acetonitrile (10 mL), and the mixture was heated at 60 °C for 4 h and then refluxed for a further 4 h. The solvent was removed in vacuum and the dark residue suspended overnight in a solution of $[NEt_4]Cl$ (0.5 g) in MeOH (10 mL). The microcrystalline precipitate was collected by filtration, washed with 2-propanol (2 × 5 mL), dried, and extracted from the frit with 6 mL of acetone. Layering with 2-propanol yielded 0.41 g (48%) of $[NEt_4]_2[Fe_2Ir_4(CO)_{16}]$. Anal. Calc for $C_{32}Fe_2H_{40}Ir_4N_2O_{16}$: C, 24.18; H, 2.51; N, 1.76. Found: C, 23.95; H, 2.40; N, 1.66.

(b) $Na_2[Fe(CO)_4]$ (0.66 g; 3.1 mmol) and $Ir_4(CO)_{12}$ (0.85 g; 0.77 mmol) were suspended in thf (25 mL), and the mixture was refluxed for 6 h. The solvent was then removed in vacuum and the tacky residue dissolved in MeOH (30 mL). Addition of $[NMe_3(CH_2Ph)]Cl$ (1.5 g) and water (15 mL) caused the precipitation of the desired product in microcrystalline form. The precipitate was collected by filtration, washed with water (10 mL), 2-propanol (2 × 5 mL), and thf (5 mL), and dried. The residue was extracted with acetone (10 mL), and the extract was layered with 2-propanol, yielding 0.65 g of crystals (52% based on iridium). Anal. Calc for $C_{36}Fe_2H_{32}Ir_4N_2O_{16}$: C, 26.5; H, 1.9, N, 1.7. Found: C, 26.81; H, 2.12; N, 1.42. FAB (negative ions): m/z = 1480 ($[NMe_3(CH_2Ph)][Fe_2Ir_4(CO)_{16}]^-$), 1330 ($[Fe_2Ir_4(CO)_{16}]^-$), 1330 − 28$x$ ($[Fe_2Ir_4(CO)_{16-x}]^-$) (x = 1–16).

Other salts of the dianion may be obtained by the same procedure using different tetraalkylammonium or phosphonium halides. The crystals of the mixed salt used for X-ray determination were fortuitously obtained from an incomplete metathesis between $[NEt_4]_2[Fe_2Ir_4(CO)_{16}]$ in acetone and $[NMe_3(CH_2Ph)]Cl$ in 2-propanol.

Tetraalkylammonium or $[N(PPh_3)_2]^+$ salts of **2** are soluble in acetone or acetonitrile, much less soluble in thf or MeOH, and insoluble in 2-propanol. IR spectrum of $[NEt_4]_2[Fe_2Ir_4(CO)_{16}]$ (Figure 3b): ν_{CO} 2006 (vs), 1987 (s), 1953 (m), 1912 (w), 1695 (m) cm^{-1} (acetonitrile solution).

X-ray Crystal Structure Determination of Salts 1a and 2a. Crystal data and experimental conditions for compounds **1a** and **2a** are reported in Table IV; more details are deposited as supplementary material and are similar to those reported in refs 1, 3, and 4. For compound **1a**, the last Fourier difference maps showed five peaks (labeled Ir(6)–Ir(10) in Table V) close to the metal vertices of the $[FeIr_4(CO)_{13}]^{2-}$ anion. These peaks were assigned to an 8% fraction of a hexanuclear cluster, probably $[Fe_2Ir_4(CO)_{16}]^{2-}$; the sixth vertex (coincident with Ir(3)) and the whole ligand sphere were ignored. A similar *molecular* substitutional disorder has already been observed in the crystals of $[PPh_4]_2[PtIr_4(CO)_{14}]$, and was treated similarly.[13] Consequently, the positional and thermal parameters of Ir(3), C(31), and C(32) might be slightly misevaluated, showing Ir–C bond distances of 1.67(2) and 1.76(4) Å, which are well below average.

Table IV. Crystallographic Data for $[PPh_4]_2[FeIr_4(CO)_{13}]\cdot C_4H_8O$ (**1a**) and $[NEt_4][NMe_3(CH_2Ph)][Fe_2Ir_4(CO)_{16}]$ (**2a**)

	1a	**2a**
formula	$C_{65}H_{48}FeIr_4O_{14}P_2$	$C_{34}H_{36}Fe_2Ir_4N_2O_{16}$
fw	1939.7	1609.2
crystal system	triclinic	monoclinic
space group	$P\bar{1}$ (No. 2)	$P2_1/c$ (No. 14)
a, Å	11.337(4)	10.763(2)
b, Å	13.105(4)	20.525(3)
c, Å	23.306(6)	19.345(3)
α, deg	100.04(2)	
β, deg	97.99(2)	97.36(1)
γ, deg	106.68(2)	
V, Å^3	3200(4)	4238(2)
Z	2	4
D_{calc}, g cm^{-3}	2.013	2.522
wavelength, Å	0.710 73	0.710 73
crystal decay	33% on F_o	none
temp, °C	23 ± 2	23 ± 2
μ, cm^{-1}	85.9	132.0
R^a	0.050	0.041
R_w^b	0.053	0.047

^{a} $R = \sum||F_o| - k|F_c||/\sum|F_o|$. ^{b} $R_w[\sum w(|F_o| - k|F_c|)^2/\sum w|F_o|^2]^{1/2}$.

(15) Shriver, D. F., Drezdzon, M. A. *The Manipulation of Air-Sensitive Compounds*, 2nd ed.; Wiley: New York, 1986.

(16) Della Pergola, R.; Garlaschelli, L.; Martinengo, S. *J. Organomet. Chem.* **1987**, *331*, 271.

(17) Strong, H.; Krusic, P. J.; San Filippo, J. *Inorg. Synth.* **1986**, *24*, 157.

(18) Farmery, K.; Kilner, M.; Greatrex, R.; Greenwood, N. N. *J. Chem. Soc. A* **1969**, 2339.

Table V. Selected Fractional Atomic Coordinates for $[PPh_4]_2[FeIr_4(CO)_{13}]\cdot C_4H_8O$ (**1a**) (Esd's in Parentheses)

atom	x	y	z
Ir(1)	0.3549(1)	0.65764(8)	0.75122(5)
Ir(2)	0.2551(1)	0.46469(8)	0.78701(4)
Ir(3)	0.21438(9)	0.47493(8)	0.66888(4)
Ir(4)	0.1071(1)	0.58242(8)	0.74948(5)
Fe(5)	0.4343(3)	0.4771(3)	0.7288(2)
O(11)	0.516(2)	0.795(2)	0.8692(9)
O(12)	0.523(2)	0.759(2)	0.672(1)
O(21)	0.109(2)	0.228(2)	0.7707(9)
O(22)	0.201(1)	0.548(1)	0.9060(7)
O(31)	0.024(2)	0.260(2)	0.617(1)
O(32)	0.154(2)	0.578(2)	0.570(1)
O(41)	−0.005(3)	0.694(2)	0.839(1)
O(42)	−0.141(3)	0.431(2)	0.685(1)
O(51)	0.689(2)	0.613(2)	0.746(1)
O(52)	0.500(2)	0.280(2)	0.705(1)
O(B1)	0.201(2)	0.798(2)	0.7191(9)
O(B2)	0.501(2)	0.468(2)	0.8551(9)
O(B3)	0.420(2)	0.452(1)	0.6002(9)
C(11)	0.452(3)	0.743(2)	0.824(1)
C(12)	0.456(3)	0.722(2)	0.703(1)
C(21)	0.166(3)	0.316(2)	0.775(1)
C(22)	0.226(3)	0.517(2)	0.859(1)
C(31)	0.102(3)	0.355(2)	0.643(1)
C(32)	0.177(3)	0.534(3)	0.609(2)
C(41)	0.043(3)	0.652(3)	0.806(1)
C(42)	−0.043(4)	0.485(3)	0.708(2)
C(51)	0.584(3)	0.553(3)	0.737(1)
C(52)	0.473(3)	0.362(3)	0.719(1)
C(B1)	0.208(3)	0.721(2)	0.733(1)
C(B2)	0.443(2)	0.477(2)	0.814(1)
C(B3)	0.383(2)	0.463(2)	0.647(1)
Ir(6)[a]	0.161(1)	0.524(1)	0.7685(5)
Ir(7)	0.412(1)	0.604(1)	0.8153(6)
Ir(8)	0.308(1)	0.393(1)	0.7509(5)
Ir(9)	0.463(1)	0.550(1)	0.7058(6)
Ir(10)[a]	0.308(2)	0.679(1)	0.7201(8)

[a] The atoms Ir(6)–Ir(10) belong to the cocrystallized unit (see text).

Table VI. Selected Fractional Atomic Coordinates for $[NEt_4][NMe_3CH_2Ph][Fe_2Ir_4(CO)_{16}]$ (**2a**) (Esd's in Parentheses)

atom	x	y	z
Ir(1)	0.90252(8)	0.17737(4)	0.55129(4)
Ir(2)	0.65069(8)	0.20944(4)	0.53213(4)
Ir(3)	0.71105(8)	0.33952(4)	0.54471(4)
Ir(4)	0.9633(1)	0.30668(5)	0.55773(5)
Fe(5)	0.8016(2)	0.26168(8)	0.44530(9)
Fe(6)	0.8073(2)	0.25614(9)	0.6450(1)
O(11)	1.146(2)	0.133(1)	0.631(1)
O(12)	0.875(2)	0.0515(7)	0.469(1)
O(21)	0.403(2)	0.229(1)	0.579(1)
O(22)	0.580(2)	0.0755(8)	0.484(1)
O(31)	0.486(2)	0.3798(9)	0.608(1)
O(32)	0.710(2)	0.4636(8)	0.464(1)
O(41)	1.200(2)	0.286(1)	0.651(1)
O(42)	1.028(2)	0.439(1)	0.512(2)
O(51)	0.800(2)	0.1593(8)	0.3422(9)
O(52)	0.822(2)	0.365(1)	0.348(1)
O(61)	0.609(2)	0.262(1)	0.7337(9)
O(62)	1.002(2)	0.2458(9)	0.7639(9)
O(B1)	0.768(2)	0.1149(7)	0.6646(8)
O(B2)	1.085(2)	0.2402(8)	0.4409(9)
O(B3)	0.531(2)	0.2818(9)	0.4006(9)
O(B4)	0.866(1)	0.3966(7)	0.6740(8)
C(11)	1.056(2)	0.152(1)	0.606(1)
C(12)	0.884(2)	0.098(1)	0.499(1)
C(21)	0.493(2)	0.221(1)	0.564(1)
C(22)	0.610(2)	0.127(1)	0.500(1)
C(31)	0.570(2)	0.363(1)	0.582(1)
C(32)	0.710(3)	0.417(1)	0.496(1)
C(41)	1.111(3)	0.294(1)	0.616(2)
C(42)	1.001(2)	0.382(1)	0.531(1)
C(51)	0.799(2)	0.200(1)	0.382(1)
C(52)	0.817(3)	0.325(1)	0.389(2)
C(61)	0.679(2)	0.259(1)	0.699(1)
C(62)	0.932(2)	0.249(1)	0.718(1)
C(B1)	0.787(2)	0.161(1)	0.634(1)
C(B2)	0.996(2)	0.249(1)	0.473(1)
C(B3)	0.624(3)	0.271(1)	0.441(1)
C(B4)	0.844(2)	0.3511(9)	0.638(1)

A certain degree of *site* substitutional disorder was observed in compound **2a** between the Fe and the Ir sites, similar to that observed in the crystal structures of ref 1. Several refinements of the occupancy factors of the metal atoms were performed, keeping the occupancy factors for all the atoms of the ligands and of the cations unitary. The refined values were then used for computing mixed-atom scattering factors, which were subsequently introduced in the final least-squares refinement cycles as follows: 95% Ir + 5% Fe for the sites labeled as Ir(1), Ir(2), and Ir(3), 70% Ir + 30% Fe for site Ir(4), 25% Ir + 75% Fe for site Fe(5), and 20% Ir + 80% Fe for site Fe(6). From the aforementioned values, it can be seen that the two Fe-rich sites are *trans* located in the M_6 octahedron; the smaller Fe fractions in the other sites can in principle be attributed to two different factors: (i) the presence of a small amount of *cis* isomers of the Fe_2Ir_4 moiety and (ii) the orientational disorder of the whole anion which, if a highly idealized symmetry (T_d) is assumed, experiences almost the same packing forces for different orientations of the metal core.

Anisotropic thermal parameters were assigned to all metal and phosphorus atoms of the two compounds and to the carbonyls and nitrogen atoms of compound **2a**. The remaining lighter O and C atoms were assigned isotropic thermal factors. The contribution of the hydrogen atoms of the cationic moieties of both compounds was ignored. The highest peaks in the final difference Fourier maps were 0.8 and 0.9 e/Å^3, mostly located in proximity to the metallic frameworks.

The final values of the positional parameters of the atoms of **1a** and **2a** are reported in Tables V and VI, respectively.

Supplementary Material Available: A detailed list of crystallographic parameters (Table S1), full lists of atomic coordinates (Tables S2 (**1a**) and S3 (**2a**)), lists of anisotropic thermal factors (Tables S4 (**1a**) and S5 (**2a**)), and full lists of distances and angles (Tables S6 (**1a**) and S7 (**2a**)) (27 pages). Ordering information is given on any current masthead page.